
CONVDTW-ACS: AUDIO SEGMENTATION FOR TRACK TYPE DETECTION DURING CAR MANUFACTURING

Álvaro López-Chilet
PRHLT Research Center
Universitat Politècnica de València
 Valencia, Spain
 allochi@upv.es

Zhaoyi Liu
imec-Distrinet
KU Leuven
 Leuven, Belgium
 zhaoyi.liu@kuleuven.be

Jon Ander Gómez
PRHLT Research Center
Universitat Politècnica de València
 Valencia, Spain
 jon@upv.es

Carlos Alvarez
Launch Department
Ford Motor Company
 Valencia, Spain
 calvare5@ford.com

Marivi Alonso Ortiz
Quality Department
Ford Motor Company
 Valencia, Spain
 malonsoo@ford.com

Andres Orejuela Mesa
Quality Department
Ford Motor Company
 Valencia, Spain
 aorejuel@ford.com

David Newton
Office of the CIO - Security & Strategy
Ford Motor Company
 Cologne, Germany
 dnewton@ford.com

Friedrich Wolf-Monheim
Ford Research & Advanced Engineering
Ford Motor Company
 Aachen, Germany
 fwolf5@ford.com

Sam Michiels
imec-Distrinet
KU Leuven
 Leuven, Belgium
 sam.michiels@kuleuven.be

Danny Hughes
imec-Distrinet
KU Leuven
 Leuven, Belgium
 danny.hughes@kuleuven.be

ABSTRACT

This paper proposes a method for Acoustic Constrained Segmentation (ACS) in audio recordings of vehicles driven through a production test track, delimiting the boundaries of surface types in the track. ACS is a variant of classical acoustic segmentation where the sequence of labels is known, contiguous and invariable, which is especially useful in this work as the test track has a standard configuration of surface types. The proposed ConvDTW-ACS method utilizes a Convolutional Neural Network for classifying overlapping image chunks extracted from the full audio spectrogram. Then, our custom Dynamic Time Warping algorithm aligns the sequence of predicted probabilities to the sequence of surface types in the track, from which timestamps of the surface type boundaries can be extracted. The method was evaluated on a real-world dataset collected from the Ford Manufacturing Plant in Valencia (Spain), achieving a mean error of 166 milliseconds when delimiting, within the audio, the boundaries of the surfaces in the track. The results demonstrate the effectiveness of the proposed method in accurately segmenting different surface types, which could enable the development of more specialized AI systems to improve the quality inspection process.

Keywords Audio Segmentation · Deep Learning · Dynamic Time Warping · Car Manufacturing · Industry 4.0, Real-world Data

1 Introduction

Artificial Intelligence (AI) is a vital tool in modern manufacturing, particularly in Industry 4.0. By leveraging technologies like 5G (Sigov et al. 2022), interconnected devices facilitate real-time data collection, analysis, and predictions.

One significant application of AI in vehicle manufacturing is process automation, leading to increased efficiency and cost reduction. A critical research area focuses on detecting and analyzing faults in quality control (Webert et al. 2022). This study centres on the quality inspection phase at the Ford Valencia Manufacturing Plant, aiming to develop a system that identifies vehicles deviating from established quality standards. A sound evaluation test is conducted post-assembly on a standardized track with various surfaces simulating different driving conditions. Skilled personnel listen for abnormal sounds indicating manufacturing defects. Automating this test requires a robust AI model to achieve high performance. Developing a segmentation model to categorize audio data by surface type enables more effective operation of specialized fault detection systems.

In this work, we present ConvDTW-ACS, a method to automatically detect the boundaries between different track surfaces given the audio of a test track run. This is an Acoustic Constrained Segmentation (ACS) task where the sequence of segments is known, contiguous and invariant, as all the recordings are collected in the same track. Therefore, the proposed method exploits this constraint to generate a better segmentation. First, a spectrogram is extracted from the whole audio. Second, a sequence of overlapping patches (*chunks*) are extracted along the time axis of the spectrogram. Then, a Convolutional Neural Network (CNN) classifies the chunks into their corresponding surface label. Finally, a constrained variant of the Dynamic Time Warping algorithm for ACS (ACS-DTW) is used to align the model predictions to the sequence of surfaces in the track, correcting errors and improving the segmentation.

The main contributions of this work are:

- A method called ConvDTW-ACS for ACS. It is designed to take into account the constraints of the task to create a more precise segmentation.
- The model is evaluated using real-world data obtained during production at the Ford Manufacturing Plant in Valencia (Spain).
- A review of the hyperparameter optimization results is presented to analyze the impact on the performance of different data preprocessing configurations, model sizes and training techniques.

The rest of the paper is organized as follows: Section 2 introduces some of the related techniques in the state-of-the-art. Section 3 gives a full description of the problem and the proposed method. Section 4 describes the dataset, metrics and tools used for experimentation. Section 5 shows the results obtained and the exploration of hyperparameters carried out. Finally, section 6 presents our conclusions.

2 Related Work

In this section, we discuss some of the related tasks that can be found in literature, highlighting their similarities with ACS.

Sound Event Detection (SED) is a task that involves identifying a class of sound events and estimating the time position (i.e. start and end) of each occurrence of that class in an audio recording. Applications of SED include detecting noise sources in urban areas (Bello et al. 2019), sound-based home monitoring (Martín-Morató and Mesáros 2023), and detecting anomalous machine sounds from manufacturing systems (Chen et al. 2023).

The conventional approach to building automatic SED systems, especially automatic sound annotation, is to train a machine learning model with labelled data. Traditional methods include Gaussian Mixture Models (GMM) (Vuegen et al. 2013), Decision Trees (Lavner and Ruinskiy 2009), Hidden Markov Models (HMM) (Heittola et al. 2013), and Support Vector Machines (SVM) (Portelo et al. 2009). Recent SED systems often use Deep Neural Networks (DNN) (Zhao et al. 2022; Ronchini and Serizel 2022), which are currently the state-of-the-art. In Venkatesh, Moffat, and Miranda 2022, the authors proposed a method that divides the spectrogram into chunks of 0.303 seconds and applies spectrogram data augmentation (*SpecAument*). They employ a Convolutional RNN model and perform a postprocessing step to remove spurious events. Martín-Morató, Harju, et al. 2023 uses soft labels for SED and explores their benefits in capturing label distribution details and improving system performance in detecting missed sounds compared to hard labels.

In addition to SED, there are other related tasks, such as Audio Segmentation and Speaker Diarization. **Audio Segmentation** involves segmenting audio data into meaningful segments, often combined with other tasks. Deep

Neural Networks (DNNs) are prevalent in state-of-the-art works, but end-to-end models are not commonly used; instead, postprocessing modules are frequently employed (Aggarwal et al. 2022). In Gimeno et al. 2020, the authors segment classes like speech, music, and noise using Mel spectrograms along with chroma features and first/second-order derivatives of the features to include audio dynamics. They train a Conv1D model with Bidirectional LSTM and use an HMM for postprocessing, employing MixUp data augmentation. In **Speaker Diarization**, similar techniques are used. State-of-the-art approaches (Park et al. 2022) typically employ DNNs for processing audio segments, followed by a post-processing step using methods such as the Viterbi algorithm (Kenny, Reynolds, and Castaldo 2010) or Bayesian Hidden Markov Models (BHMM) (Diez et al. 2020) to obtain the final prediction.

In the proposed ACS-DTW custom algorithm, step constraints are added to better align the model predicted probabilities with the known surface types order and their expected duration. These kind of restrictions have been previously applied in Speech Segmentation. In Gómez, Sanchis, and Castro-Bleda 2010, phonetic boundaries are detected using Acoustical Clustering-Dynamic Time Warping (AC-DTW), using the predicted probabilities of a GMM.

3 Proposed Method

This section presents first the problem description and then a complete revision of our proposed method.

3.1 Problem Description

In car manufacturing, after a vehicle is fully assembled it needs to pass several test phases to validate that the product meets the quality standards. Once the car exits the production line, fully assembled, it has to pass a drive test where different checks are performed. One of the main tests during this drive is to look for possible anomalous sounds that could be produced by a manufacturing defect. The test track where this final validation is performed has different kinds of surfaces. Each of these surfaces is designed to test specific driving conditions, from normal to more extreme situations. Therefore, anomalous sounds may appear in some surfaces and not in others.

The process timing is also very important when dealing with a complex and big production line that assembles hundreds of vehicles a day. Because of this, the inference time of the ACS system must be small, as it is going to be usually executed before other systems (e.g. sound anomaly detection).

The main difference between ACS and other typical segmentation tasks (e.g. music and speech detection (Aggarwal et al. 2022) or speaker diarization (Park et al. 2022)) is that we know in advance which is the sequence of labels (surfaces) and that they are contiguous. In the end, the system should provide a list of boundaries separating the different surfaces of the track.

3.2 Method Overview

In this section we introduce the main blocks of ConvDTW-ACS to exploit the constraints of ACS. In order to predict the surface boundaries, the system proposed uses a Convolutional Neural Network (CNN) to perform audio classification over spectrogram segments, which we refer to as *chunks*. For each chunk a surface label is assigned to train the classifier. Then, a postprocessing step using a variant of DTW is applied over the sequence of model predictions to get the final segmentation. In Figure 1 a complete diagram of ConvDTW-ACS is shown.

To explain the method in more detail, it can be divided into three main blocks:

1. **Data preprocessing:** Extracts a spectrogram from the raw waveform and generates fixed size chunks from it. The chunks are extracted along the time axis with overlap between them.
2. **CNN classifier:** Performs the test track surface classification for each spectrogram chunk. This creates a sequence of probability vectors with a preliminary segmentation.
3. **ACS-DTW Segmentation Postprocessing:** This block is the main component for ACS. Applies a custom variant of the Dynamic Time Warping (DTW) algorithm over the model predictions to correct and improve the segmentation. This optimization takes into account the order of the surfaces in the track to get the best alignment with the predictions. Therefore, chunk classification errors produced by the CNN model are corrected and the surface boundaries improved.

In the following sections each pipeline block is explained in detail.

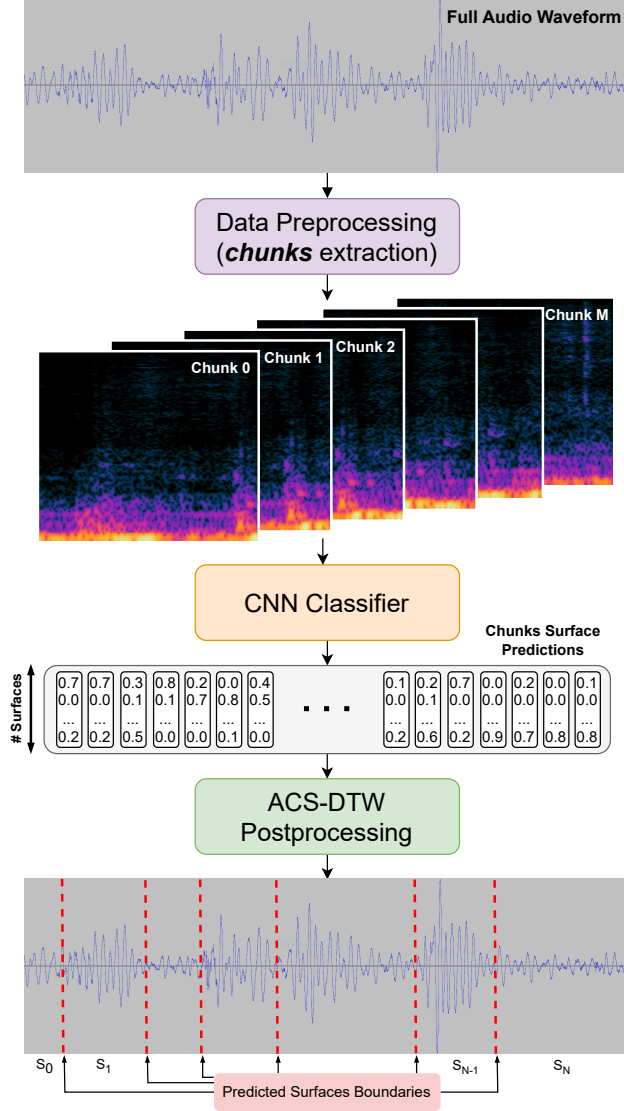


Figure 1: Diagram of the proposed ConvDTW-ACS method. First, the raw waveform is preprocessed to extract the spectrogram chunks. Then, a CNN model is used to classify each chunk among all the surfaces. Finally, our ACS-DTW algorithm is applied to align the model predictions to the order of the surfaces in the track. This produces the final segmentation composed by the boundary timestamps between surfaces.

3.3 Data Preprocessing

The duration of one audio in the test track lasts about 2 minutes, including some out-of-track time where the car enters and leaves the track. This duration depends both on the speed of the driver and possible stops due to traffic or other production conditions. To deal with this long and variable audio samples, a chunk-based preprocessing is performed to get fixed size windows of data and process the whole signal.

From the raw WAV file data to the final input data tensors feed to the model, our data loading pipeline performs the following steps (shown in Figure 2):

1. **Waveform preprocessing:** First, the full waveform data is loaded. Then, in the experiments with waveform data augmentation, the following transformations from the *audiomentations* (Jordal et al. 2023) library were randomly applied: *AirAbsorption*, *AddGaussianSNR*, *ClippingDistortion*. After the augmentations, the *Normalize* transform is used to obtain always data in the same range $[-1, 1]$.

2. **Wave to spectrogram:** It is well-established that transforming waveform data from the amplitude domain to the frequency domain can result in a better feature extraction (Park et al. 2022; Aggarwal et al. 2022). In our experiments, we tried three different spectrogram extractions from the *torchaudio* (Yang et al. 2021) library: *Spectrogram*, *MelSpectrogram* and *MFCC*.
3. **Chunks extraction:** After getting the spectrogram of the whole audio, we extract chunks of fixed size to get the input samples for the model. The extraction is controlled by two hyperparameters: *chunk_size*, that determines the width of the chunk; and *chunk_hop*, that determines the displacement between chunks (see Figure 2). The *chunk_hop* controls the overlapping between chunks and determines the segmentation resolution. Where smaller values of it increase the resolution at the cost of increasing the number of chunks and the computational cost. Finally, to get the test track’s surface label for each chunk, we take the label at the timestamp of the middle frame of the chunk, as more than one surface may appear in a chunk. In the experiments with data augmentation, we also use *MixUp* (Zhang et al. 2017) among the chunks of each training batch.

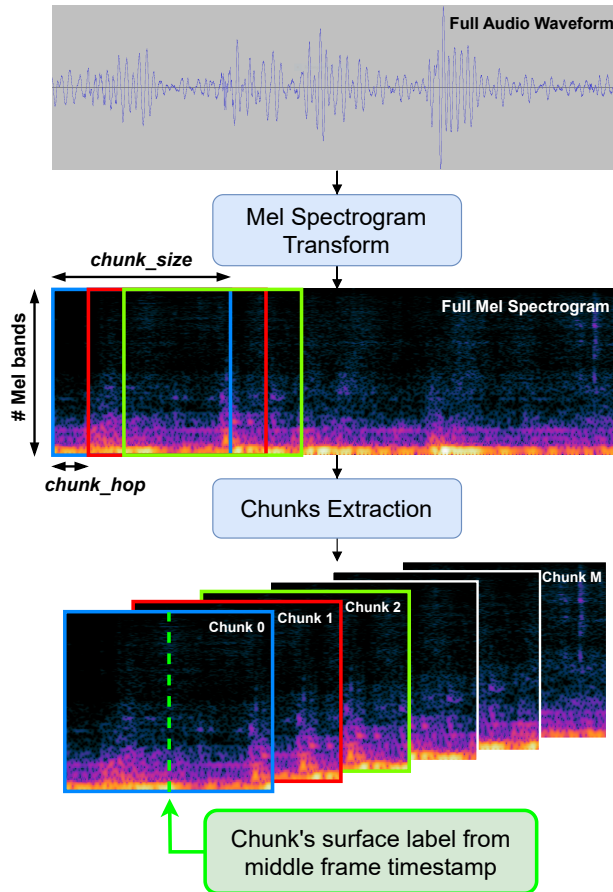


Figure 2: Diagram of the data preprocessing pipeline using the Mel spectrogram as feature extraction. It shows how the input samples (*chunks*) for the CNN classifier are extracted from the raw audio waveform. The dimensions of each chunk image are ($channels = 1, height = Mel\ bands, width = chunk_size$). For each chunk a surface label is assigned taking into account the middle frame of the chunk, generating the ground-truth for the CNN classifier.

3.4 CNN Classifier

Once all the M chunks are extracted from the full audio sample, we perform a classification step to get M predictions. All the chunks are fed into a CNN to classify among all the possible surfaces. The CNN architecture used is the *ResNet* (He et al. 2015), where all the different size variants have been tried. We used this architecture as it is a well established baseline for image classification and the size of the model is appropriate for the number of samples in the dataset. Pretrained *Imagenet* (Russakovsky et al. 2014) weights from the *torchvision* library (Marcel and Rodriguez 2010) have been used to improve the training process. To adapt the pretrained model architecture to our task, first, we

added zero padding to our one-channel image chunks to fit the 3-channel input (for RGB images), then, we removed the fully connected layer from the original model and we added our own classifier composed by: *BatchNorm* and *Linear(units=2048)* layers, followed by *BatchNorm*, *ReLU*, *Dropout(p=0.4)* and the output *Linear(units=17)* layer with *Softmax* activation function.

As a result of this classification over all the chunks in an audio sample, we get a sequence of model predictions where we keep the probabilities for each class. Each prediction corresponds to the middle frame’s timestep of each chunk. So we get a prediction every *chunk_hop* frames, which defines the resolution of our segmentation.

3.5 ACS-DTW Segmentation Postprocessing

The preliminary segmentation generated by the CNN model can contain some errors due to the fact that the model is not taking into account the order of the surfaces in the track. As this model is a classifier among all the surfaces but agnostic to the chronological order, given a chunk at time m classified as belonging to the surface n , the model can classify the next chunk as any surface type, even the previous ones, when the unique valid surface labels are n and $n + 1$. Only these kind of operations are the possible ones due to the nature of the use case, where all the surfaces must appear in the correct order. Another problem generated by spontaneous misclassifications is that very short segments may appear, even with a duration of a single chunk. In this final step of the pipeline, we avoid these kind of errors in order to select the optimal surface boundaries. To accomplish this, we take into account the real sequence of surfaces and a minimum duration per surface.

The proposed method to generate the final segmentation is a dynamic programming algorithm with limited rules to (i) avoid assigning several labels to the same chunk while (ii) allowing that a subsequence of consecutive chunks are assigned to the same label. This is known as the Dynamic Time Warping (DTW). The original DTW compares two signals with different duration, x and y , and returns an alignment between their elements based on a cost function which is usually minimized. In our case, we want to align the sequence of surfaces, x , in the track with the surface probabilities, y , predicted by the model, which is a sequence of predicted class probabilities for each chunk. The goal is to assign the final track label to each chunk by taking into account the real order of the surfaces. Consequently, the algorithm fills a cost matrix $D_{N \times M}$ by accumulating a cost function c , where N is the number of surfaces and M the number of chunks. And once D is computed, the solution path can be extracted to get the alignment between the two sequences x and y . In our case, this alignment assigns a surface label from x to each chunk in y . Our cost function is the logarithm of the output probability of the CNN model for a given surface x_n and chunk y_m : $c(x_n, y_m) = \log P(\text{surface} = n | \text{chunk} = m)$. Therefore, we maximize c instead of minimizing it as the typical approach. In “Dynamic Time Warping” 2007, variations of the original DTW are presented to force the algorithm to take more suitable paths. Our proposed ACS-DTW is based on the variant to restrict the step function but with further modifications. These restrictions are applied to force the algorithm to set a minimum duration in chunks for each surface. Where the minimum duration per surface was extracted by computing the minimum duration of each surface in the training subset of the dataset. This duration in seconds is then converted to the corresponding number of chunks. The changes that we applied to our algorithm are the following:

- **Remove vertical alignment:** In the original DTW three kinds of steps are allowed: (1) vertical, where an element of the sequence y is aligned to more than one from x , (2) diagonal, where the elements of both sequences are aligned 1 to 1, and (3) horizontal, where an element of x is aligned to more than one from y . Due to the problem restrictions, it does not make sense to assign a chunk from y to more than one surface from x , so the vertical step is not considered in our implementation.
- **Diagonal step constraint:** As we removed the vertical step, the only way to advance to the next surface is by the diagonal move. Thus, instead of using the regular diagonal step, we applied a step function condition. This condition is that to be able to go to the next surface n , a minimum number of chunks min_chunks_n must be assigned to surface n , where min_chunks_n is the minimum number of chunks obtained from the dataset exploration for that surface n . Given this definition, the cost matrix D is computed using the Equation 1. Note that at each row n the value of min_chunks_n will be different, adjusting the condition to each surface.

$$D(n, m) = \max \begin{cases} D(n, m - 1) + c(x_n, y_m), \\ D(n - 1, m - min_chunks_n) + \sum_{i=1}^{min_chunks_n} c(x_n, y_{m-i+1}), \end{cases} \quad (1)$$

The full algorithm definition to fill the cost matrix is shown in Algorithm 1. Once we have the matrix D computed, we can retrieve the alignment to get the final label for each chunk.

Finally, after getting the final chunks labels, we can transform that into timestamps (in seconds) to set the boundaries between surfaces.

Algorithm 1 ACS Dynamic Time Warping (ACS-DTW): Definition of the algorithm to fill the D matrix. Note that the implementation of the backtrace to get the alignment is omitted for clarity.

Input: Surfaces sequence x , chunks predictions y , number of surfaces N , number of chunks M and list of minimum chunks per surface min_chunks

Output: Cost matrix D

```

1: // Initialization to maximize  $c$ 
2:  $D(0..N, 0..M) = -\inf$ 
3:
4: // Fill the first row of  $D$  (surface  $n = 0$ )
5:  $D(0, 0) = c(x_0, y_0)$ 
6: for  $m = 1$  to  $M$  do
7:    $D(0, m) = D(0, m - 1) + c(x_0, y_m)$ 
8: end for
9:
10: // To skip a min number of chunks to reach a surface
11:  $start\_chunk = min\_chunks_0 - 1$ 
12: for  $n = 1$  to  $N$  do
13:   // Add the min number of chunks to reach surface  $n$ 
14:    $start\_chunk = start\_chunk + min\_chunks_n$ 
15:   for  $m = start\_chunk$  to  $M$  do
16:
```

$$D(n, m) = \max \begin{cases} D(n, m - 1) + c(x_n, y_m), \\ D(n - 1, m - min_chunks_n) + \sum_{i=1}^{min_chunks_n} c(x_n, y_{n-i+1}), \end{cases}$$

```

17:   end for
18: end for
19: return  $D$ 
```

4 Experimental Setup

4.1 Dataset

The dataset used in this work has been collected at the Ford Manufacturing Plant in Valencia (Spain). All the audio data was recorded during production in order to get a representative dataset of the real environment.

To collect the samples a custom device was built to record audio. This device is designed to be placed in the headrest of the copilot and uses a Lavalier microphone to record mono audio. The configuration of the recording is set to use a sampling rate of 22050 Hz. And the data was stored in uncompressed WAV format to avoid any loss.

A data collection phase has been performed recording samples from the same vehicle model but with variations in terms of motorization and equipment. In total, 1823 audio samples were collected. Each of the recordings has an approximate duration of 2 minutes, including not only the audio from the track but also some additional audio before and after the track. These additional segments not belonging to the track are included because the driver starts the recording before entering the track and stops it outside the track. Nevertheless, this out-of-track segments count as a surface to detect. Because in case of using the proposed segmentation method inside a more complex pipeline, we may want to use it to remove these segments before doing any further audio analysis.

From the 1823 audio samples, we manually segmented 50 of them, by setting the exact instant of time where there is a transition between surface types. There are 17 different surfaces to detect, where two of them are corresponding to the preceding and succeeding segments not belonging to the track. As the track is completely standardized, it must be completed always at a determined speed and without stopping or changing the path. Therefore, we can take into account the constraint of always generating the sequence of surfaces in the same order and following a similar duration.

The 50 segmented audios have been selected to form a segmentation dataset, accumulating a total of 1.84 hours of audio. It was split in a train set of 42 samples and a test set of 8. Then during training, from the 42 samples, 8 were used for the validation set.

Because of the nature of the dataset the amount of data for each surface is not balanced, as the length and speed changes from one surface to other. For privacy reasons the exact distribution is not going to be shown, but to illustrate, the duration of a surface can go from 3 to 15 seconds approximately.

4.2 Metrics

The metrics used to evaluate the system can be divided in two groups:

- **Classifier Metrics:** Metrics computed to evaluate the CNN model that classifies the individual chunks among the available track surfaces, without applying ACS-DTW algorithm. The classification metrics used are accuracy and F1-score.
- **Segmentation Metrics:** Metrics computed using the final segmentation after the segmentation postprocessing has been applied using our ACS-DTW algorithm. The metrics are:
 - **Mean error:** Mean of the absolute error values when measuring distance between predicted and true surfaces boundaries.
 - **Barrier Threshold Accuracy:** Accuracy metric applied to each one of the predicted boundaries. If the error (in seconds) for a boundary is higher than the threshold it is taken as a miss, else a hit. The thresholds considered are: 0.2s, 0.5s and 1.0s. These have been selected because they represent from a highly satisfactory threshold (0.2s) to the maximum (1.0s) that we consider acceptable for the use case.

4.3 Computing Resources

The machine used to run the experiments has an Intel Xeon W-2245 CPU (8 cores), a NVIDIA RTX A6000 GPU (48 GB) and 32 GB of RAM. The batch size used is 512 as it results in the best performance.

4.4 Software

To build the pipeline several libraries have been used. Regarding data loading and preprocessing we used *librosa* (McFee et al. 2022) and *torchaudio* (Yang et al. 2021). To apply data augmentation to the waveform data we used *audiomentations* (Jordal et al. 2023). To orchestrate the training pipeline *Pytorch Lightning* (Falcon and team 2023) was used along with *Optuna* (Akiba et al. 2019) for hyperparameter optimization.

5 Results

In this section the results of our experimentation are shown. A comparison of different hyperparameters and training configurations is presented in order to analyze the impact of each variant on the CNN classifier and in the final segmentation.

To train all the experiments presented in the following tables, we used a baseline configuration with the *AdamW* optimizer (Loshchilov and Hutter 2017), a learning rate of $1e^{-4}$, and a weight decay of $6.1e^{-3}$. For feature extraction, we used the *Mel spectrogram* with 70 Mel bands, and a *chunk_hop* of 1 spectrogram frame. As for the CNN classifier, we used the *ResNet-152* CNN architecture with pretrained *Imagenet* weights. This configuration was selected using *Optuna* for hyperparameter optimization search.

Two of the most important hyperparameters to tune the performance of the system are: the size of the Fast Fourier Transform (FFT), declared as *n_fft*; and the number of spectrogram frames per chunk, declared as *chunk_size*. Note that for the spectrogram computation using FFT, we use a window overlapping of 50%. When tuning *n_fft* and *chunk_size*, the following trade-offs must be taken into account:

- ***n_fft*:** Increasing the value decreases the total number of chunks extracted from the whole spectrogram, as the *chunk_hop* gets bigger in time. This implies to reduce the resolution of the segmentation but also improves the inference time, as less chunks have to be processed.
- ***chunk_size*:** The size of this value is directly proportional to the amount of context that we want to give per chunk. Small values may not provide enough context to effectively classify a chunk, but a very large context increases memory footprint and inference time.

Table 1 presents the results of our exploration of various combinations of *n_fft* and *chunk_size*. We selected different *chunk_size* values for each *n_fft* value to ensure that the amount of context included in each chunk was approximately the same in seconds. Our results indicate that classification metrics were lower for the smallest values of *chunk_size*, which resulted in decreased segmentation performance. After evaluating all the combinations, we determined that the combination of *n_fft* = 4096 and *chunk_size* = 91 was the optimal choice, striking a balance between accuracy and performance. While the combination of *n_fft* = 2048 and *chunk_size* = 121 resulted in a slight increase in precision, the cost was much higher, as it generates twice as many chunks and with higher size. The maximum chunk size in

seconds is approximately 8.4, because in case of larger chunks, samples of the final class would not be generated due to the offset of the extraction window. Since there would be audios in which the duration of the last surface is less than half a chunk.

Table 1: Comparison of different sizes for the FFT computation (n_fft) in spectrogram transform and $chunk_size$ values. The $chunk_size$ is adjusted for each value of n_fft to take a similar context window (in seconds).

n_fft	$chunk_size$	Chunk Acc.	Chunk F1	Mean err. (s)	Barrier Threshold Acc.		
					0.2s	0.5s	1.0s
1024	81 (1.88s)	0.76	0.73	0.257	0.75	0.83	0.93
	161 (3.74s)	0.83	0.83	0.180	0.79	0.89	0.95
	241 (5.60s)	0.85	0.84	0.204	0.75	0.87	0.95
	281 (6.52s)	0.82	0.82	0.202	0.78	0.89	0.94
	321 (7.45s)	0.85	0.84	0.193	0.79	0.87	0.95
	361 (8.38s)	0.87	0.87	0.166	0.76	0.89	0.98
2048	41 (1.90s)	0.73	0.70	0.310	0.67	0.83	0.91
	81 (3.76s)	0.85	0.84	0.197	0.76	0.90	0.96
	121 (5.62s)	0.86	0.85	0.157	0.82	0.91	0.97
	141 (6.55s)	0.85	0.83	0.271	0.76	0.87	0.92
	161 (7.48s)	0.87	0.86	0.299	0.78	0.88	0.95
	181 (8.41s)	0.88	0.86	0.181	0.81	0.90	0.98
4096	21 (1.95s)	0.72	0.67	0.261	0.68	0.85	0.96
	41 (3.81s)	0.83	0.81	0.303	0.69	0.88	0.94
	61 (5.67s)	0.85	0.83	0.230	0.68	0.90	0.96
	71 (6.59s)	0.88	0.86	0.226	0.73	0.92	0.96
	81 (7.52s)	0.89	0.88	0.180	0.76	0.93	0.98
	91 (8.45s)	0.91	0.90	0.178	0.77	0.90	0.99
8192	11 (2.04s)	0.54	0.53	0.480	0.53	0.74	0.86
	21 (3.90s)	0.71	0.67	0.423	0.55	0.77	0.88
	31 (5.76s)	0.83	0.81	0.362	0.61	0.86	0.91
	35 (6.50s)	0.82	0.82	0.376	0.62	0.85	0.94
	41 (7.61s)	0.86	0.86	0.408	0.64	0.84	0.94
	45 (8.36s)	0.87	0.86	0.240	0.65	0.90	0.97

After analyzing the chunk extraction parameters, we determined that the optimal combination is $n_fft = 4096$ and $chunk_size = 91$, from this baseline, we further investigated how different sizes of our model could affect performance. In previous experiments, we used the largest variant, *ResNet-152*. In Table 2, we present the results of our experiments using smaller versions of *ResNet*. Interestingly, the best results were obtained using the smallest variant, *ResNet-18*. This suggests that using a model with fewer parameters can improve performance without sacrificing accuracy.

Table 2: Comparison of the different ResNet model variants with pretrained weights. All the experiments were run with the same data preprocessing and training configuration ($n_fft = 4096$ and $chunk_size = 91$).

ResNet	Chunk Accuracy	Chunk F1	Mean err. (s)	Barrier Threshold Acc.		
				0.2s	0.5s	1.0s
18	0.92	0.92	0.174	0.73	0.90	1.0
34	0.92	0.91	0.202	0.73	0.90	0.96
50	0.85	0.84	0.347	0.63	0.83	0.94
101	0.89	0.88	0.257	0.70	0.81	0.97
152	0.91	0.90	0.178	0.77	0.90	0.99

We explored the *ResNet* architectures using pretrained weights from *Imagenet* as a baseline. It has been demonstrated that transfer learning using *Imagenet* weights can improve results even in different domains (Yamada and Otani 2022). However, we also compared the results using the same *ResNet-18* architecture trained from scratch and found that using pretrained weights consistently improved the training results (Table 3).

In addition to the Mel spectrogram, which we used to extract frequency-domain features, we explored two other transformations: the *Base* spectrogram, which was extracted using the Short Time Fourier Transform (STFT), and

Table 3: Comparison of using a *ResNet-18* with pretrained weights and without.

Pretrained Weights	Chunk Accuracy	Chunk F1	Mean err. (s)	Barrier Threshold Acc.		
				0.2s	0.5s	1.0s
Yes (Imagenet)	0.92	0.92	0.174	0.73	0.90	1.0
No	0.90	0.91	0.188	0.70	0.93	0.97

Mel-Frequency Cepstrum Coefficients (*MFCC*), which were extracted using 40 coefficients. Table 4 presents the results of our experiments with these different spectrograms. We found that the *MFCC* method resulted in significantly worse classification metrics for the chunks and a high segmentation error, indicating that it is not suitable for this task. As for the other two methods, *Base* and *Mel*, we obtained similar results in terms of segmentation accuracy with no clear best option. However, considering inference time and memory footprint, the Mel spectrogram is a better option, as it generates chunks that are much smaller.

Table 4: Comparison of different transforms to extract a spectrogram from the waveform data. Where *Base* represents the Short Time Fourier Transform (STFT) spectrogram, *Mel* the Mel spectrogram using 70 Mel bands, and *MFCC* the Mel-Frequency Cepstrum Coefficients with 40 coefficients.

Spectrogram	Chunk Accuracy	Chunk F1	Mean err. (s)	Barrier Threshold Acc.		
				0.2s	0.5s	1.0s
Base	0.92	0.92	0.172	0.73	0.92	0.99
Mel	0.92	0.92	0.174	0.73	0.90	1.00
MFCC	0.56	0.57	1.945	0.41	0.60	0.71

As our dataset contains only 1.84 hours of audio, we explored different data augmentation methods to improve the training results. We experimented with waveform level transformations and *MixUp* applied to the training batches as a generic data augmentation method. Table 5 presents the results of each of these methods and their combination. We found that the accuracy metrics decreased when waveform augmentation was applied, indicating that it is not suitable for this task. However, in the case of *MixUp*, we observed that while the CNN model accuracy was lower, the segmentation precision was higher. This suggests that the probabilities given by the model are better calibrated when using *MixUp*, and as a result, the ACS-DTW algorithm can achieve a slightly more precise segmentation.

Table 5: Comparison of different Data Augmentation methods. The methods compared are: (1) No data augmentation, (2) Waveform transforms, (3) Batch MixUp, (4) Combination of waveform transforms and batch MixUp.

Data Aug.	Chunk Accuracy	Chunk F1	Mean err. (s)	Barrier Threshold Acc.		
				0.2s	0.5s	1.0s
No	0.92	0.92	0.174	0.73	0.90	1.0
Wave	0.90	0.89	0.198	0.66	0.87	0.99
MixUp	0.89	0.89	0.166	0.79	0.92	0.98
Wave + MixUp	0.88	0.89	0.281	0.71	0.90	0.97

6 Conclusions

In this work, we presented the ConvDTW-ACS method for accurately segmenting track surface types in audio recordings of vehicles driven through a production test track. Our method was evaluated on a real-world dataset collected from the Ford Manufacturing Plant in Valencia (Spain), achieving a mean error of 166 milliseconds when delimiting the boundaries of the track surfaces. These results demonstrate the effectiveness of the proposed method in accurately segmenting different surface types, enabling the application of more specialized AI systems such as Anomaly Detection to improve the quality inspection process. Moreover, we explored various hyperparameter combinations and presented their trade-offs in terms of segmentation accuracy and computational cost. Overall, our proposed method provides a promising approach for improving the efficiency and accuracy of quality inspection in vehicle production lines.

7 Acknowledgments

We would like to thank the Ford Manufacturing Plant in Valencia (Spain) for supporting this project and making this research possible. Especially, we would like to thank the Quality Department for their great involvement in the correct collection and labelling of the data; and the Launch Department for promoting and supporting the project.

This research was funded by Ford Motor Company under the Ford Manufacturing Plan in Valencia (Spain) and the KU Leuven Ford Alliance Agreement (Project: Automated Squeak & Rattle Testing, KUL0134).

References

- Aggarwal, Shruti et al. (Aug. 2022). “Audio Segmentation Techniques and Applications Based on Deep Learning”. In: *Scientific Programming* 2022. DOI: <https://doi.org/10.1155/2022/7994191>.
- Akiba, Takuya et al. (2019). “Optuna: A Next-generation Hyperparameter Optimization Framework”. In: *Proceedings of the 25th ACM SIGKDD International Conference on Knowledge Discovery and Data Mining*.
- Bello, Juan P et al. (2019). “Sonyc: A system for monitoring, analyzing, and mitigating urban noise pollution”. In: *Communications of the ACM* 62.2, pp. 68–77.
- Chen, Haihui et al. (2023). “SW-WAVENET: Learning Representation from Spectrogram and Wavegram Using Wavenet for Anomalous Sound Detection”. In: *ICASSP 2023-2023 IEEE International Conference on Acoustics, Speech and Signal Processing (ICASSP)*. IEEE, pp. 1–5.
- Diez, Mireia et al. (2020). “Optimizing Bayesian Hmm Based X-Vector Clustering for the Second Diarization Challenge”. In: *ICASSP 2020 - 2020 IEEE International Conference on Acoustics, Speech and Signal Processing (ICASSP)*, pp. 6519–6523. DOI: 10.1109/ICASSP40776.2020.9053982.
- Dynamic Time Warping* (2007). In: *Information Retrieval for Music and Motion*. Berlin, Heidelberg: Springer Berlin Heidelberg, pp. 69–84. ISBN: 978-3-540-74048-3. DOI: 10.1007/978-3-540-74048-3_4. URL: https://doi.org/10.1007/978-3-540-74048-3_4.
- Falcon, William and The PyTorch Lightning team (Mar. 2023). *PyTorch Lightning*. Version 2.0.0. DOI: 10.5281/zenodo.7737218. URL: <https://doi.org/10.5281/zenodo.7737218>.
- Gimeno, Pablo et al. (Mar. 2020). “Multiclass audio segmentation based on recurrent neural networks for broadcast domain data”. In: *EURASIP Journal on Audio, Speech, and Music Processing* 2020.1, p. 5. DOI: <https://doi.org/10.1186/s13636-020-00172-6>.
- Gómez, Jon A., Emilio Sanchis, and María J. Castro-Bleda (2010). “Automatic Speech Segmentation Based on Acoustical Clustering”. In: *Structural, Syntactic, and Statistical Pattern Recognition*. Ed. by Edwin R. Hancock et al. Berlin, Heidelberg: Springer Berlin Heidelberg, pp. 540–548. ISBN: 978-3-642-14980-1.
- He, Kaiming et al. (2015). “Deep Residual Learning for Image Recognition”. In: *CoRR* abs/1512.03385. arXiv: 1512.03385. URL: <http://arxiv.org/abs/1512.03385>.
- Heittola, Toni et al. (2013). “Context-dependent sound event detection”. In: *EURASIP Journal on audio, speech, and music processing* 2013.1, pp. 1–13.
- Jordal, Iver et al. (June 2023). *iver56/audiomentations: v0.31.0*. DOI: 10.5281/zenodo.8063135.
- Kenny, Patrick, Douglas Reynolds, and Fabio Castaldo (2010). “Diarization of Telephone Conversations Using Factor Analysis”. In: *IEEE Journal of Selected Topics in Signal Processing* 4.6, pp. 1059–1070. DOI: 10.1109/JSTSP.2010.2081790.
- Lavner, Yizhar and Dima Ruinskiy (Jan. 2009). “A Decision-Tree-Based Algorithm for Speech/Music Classification and Segmentation”. In: *EURASIP J. Audio, Speech and Music Processing* 2009. DOI: 10.1155/2009/239892.
- Loshchilov, Ilya and Frank Hutter (2017). “Fixing Weight Decay Regularization in Adam”. In: *CoRR* abs/1711.05101. arXiv: 1711.05101. URL: <http://arxiv.org/abs/1711.05101>.
- Marcel, Sébastien and Yann Rodriguez (2010). “Torchvision the machine-vision package of torch”. In: *Proceedings of the 18th ACM international conference on Multimedia*. URL: <https://api.semanticscholar.org/CorpusID:24961049>.
- Martín-Morató, Irene, Manu Harju, et al. (2023). “Training sound event detection with soft labels from crowdsourced annotations”. In: *ICASSP 2023-2023 IEEE International Conference on Acoustics, Speech and Signal Processing (ICASSP)*. IEEE, pp. 1–5.
- Martín-Morató, Irene and Annamaria Mesaros (2023). “Strong labeling of sound events using crowdsourced weak labels and annotator competence estimation”. In: *IEEE/ACM Transactions on Audio, Speech, and Language Processing* 31, pp. 902–914.
- McFee, Brian et al. (June 2022). *librosa/librosa: 0.9.2*. Version 0.9.2. DOI: 10.5281/zenodo.6759664. URL: <https://doi.org/10.5281/zenodo.6759664>.
- Park, Tae Jin et al. (2022). “A review of speaker diarization: Recent advances with deep learning”. In: *Computer Speech & Language* 72, p. 101317. ISSN: 0885-2308. DOI: <https://doi.org/10.1016/j.cs1.2021.101317>.

- Portelo, Jose et al. (2009). “Non-speech audio event detection”. In: *2009 IEEE International Conference on Acoustics, Speech and Signal Processing*. IEEE, pp. 1973–1976.
- Ronchini, Francesca and Romain Serizel (2022). “A benchmark of state-of-the-art sound event detection systems evaluated on synthetic soundscapes”. In: *ICASSP 2022-2022 IEEE International Conference on Acoustics, Speech and Signal Processing (ICASSP)*. IEEE, pp. 1031–1035.
- Russakovsky, Olga et al. (2014). “ImageNet Large Scale Visual Recognition Challenge”. In: *CoRR* abs/1409.0575. arXiv: 1409.0575. URL: <http://arxiv.org/abs/1409.0575>.
- Sigov, Alexander et al. (Jan. 2022). “Emerging Enabling Technologies for Industry 4.0 and Beyond”. In: *Information Systems Frontiers*. ISSN: 1572-9419. DOI: 10.1007/s10796-021-10213-w. URL: <https://doi.org/10.1007/s10796-021-10213-w>.
- Venkatesh, Satvik, David Moffat, and Eduardo Reck Miranda (2022). “You Only Hear Once: A YOLO-like Algorithm for Audio Segmentation and Sound Event Detection”. In: *Applied Sciences* 12.7. ISSN: 2076-3417. DOI: 10.3390/app12073293. URL: <https://www.mdpi.com/2076-3417/12/7/3293>.
- Vuegen, Lode et al. (2013). “An MFCC-GMM approach for event detection and classification”. In: *IEEE workshop on applications of signal processing to audio and acoustics (WASPAA)*, pp. 1–3.
- Webert, Heiko et al. (2022). “Fault Handling in Industry 4.0: Definition, Process and Applications”. In: *Sensors* 22.6. ISSN: 1424-8220. DOI: 10.3390/s22062205. URL: <https://www.mdpi.com/1424-8220/22/6/2205>.
- Yamada, Yutaro and Mayu Otani (June 2022). “Does Robustness on ImageNet Transfer to Downstream Tasks?” In: *Proceedings of the IEEE/CVF Conference on Computer Vision and Pattern Recognition (CVPR)*, pp. 9215–9224.
- Yang, Yao-Yuan et al. (2021). “TorchAudio: Building Blocks for Audio and Speech Processing”. In: *arXiv preprint arXiv:2110.15018*.
- Zhang, Hongyi et al. (2017). “mixup: Beyond Empirical Risk Minimization”. In: *CoRR* abs/1710.09412. arXiv: 1710.09412. URL: <http://arxiv.org/abs/1710.09412>.
- Zhao, Xujiang et al. (2022). “Seed: Sound event early detection via evidential uncertainty”. In: *ICASSP 2022-2022 IEEE International Conference on Acoustics, Speech and Signal Processing (ICASSP)*. IEEE, pp. 3618–3622.